Methods for Evaluating Explosion Resistant Ventilation Structures

M J Sapko[1], E S Weiss[1] and S P Harteis[1]

ABSTRACT

The Pittsburgh Research Laboratory (PRL) of the National Institute for Occupational Safety and Health (NIOSH) has conducted full-scale explosion experiments, to evaluate the strength characteristics of various seal designs, used for safely isolating worked-out areas in underground coal mines. Large-scale explosion tests conducted within the multiple entry section of PRL's Lake Lynn Experimental Mine (LLEM) is currently the only accepted test method used by the Mine Safety and Health Administration (MSHA), for deeming a seal design suitable for use in American mines. These explosion tests are labour intensive, expensive to conduct, and can interfere with other critical underground safety and health research programs conducted by NIOSH. The PRL has developed an alternative seal evaluation method, based on a hydrostatic pressure loading concept, that can facilitate the *in situ* testing of seals in an operating mine. Two chambers within LLEM and one within PRL's Safety Research Coal Mine (SRCM) were used for hydrostatic pressure loading various seal designs. The results from these chamber tests compare favourably with those from the large-scale explosion tests in the multiple entries. In addition to testing seal designs at the required 20 psi static pressure level, the chamber test approach also allows for the determination of the seal's ultimate design strength. Size-scaling relationships for predicting the strength of seal designs as a function of entry size are also presented.

INTRODUCTION

US mine ventilation plans require seals to protect against explosions. They are used extensively in mining to isolate worked-out areas and active fire zones. Over the years more than 30 000 seals have been erected in underground coal mines in the United States. Seals, along with generalised rock dusting and good ventilation constitute the dominant portion of America's line of defence against underground coal mine explosions. Without reliable seals, a great number of miner's lives could be in jeopardy. Within the last ten years, seven documented explosions of methane and/or coal dust occurred within sealed areas of underground US coal mines (Hurren, Tuggle and McGruder, 1993; Scott *et al*, 1996). These explosions, believed to be initiated by lightning strikes on the surface, destroyed numerous seals and caused considerable damage external to the sealed area. Fortunately, these explosions did not cause fatalities or injuries. The potential for a life-threatening disaster exists however, emphasising the need for explosion resistant seals that can perform under various mining conditions.

Title 30, Part 75.335 of the Code of Federal Regulations (30 CFR)(1995) states that abandoned areas of a mine must be either ventilated or isolated from active workings through the use of seals capable of withstanding a *static* horizontal pressure rise of 20 psi (138 kPa). Seals are also used to isolate fire zones or areas susceptible to spontaneous combustion. To effectively isolate areas within a mine, a seal should control the methane and air exchange between the sealed and open areas so as to prevent toxic and/or flammable gases from entering the active workings. A seal must be capable of preventing an explosion from propagating into, or out of the sealed area. Early US Bureau of Mines (USBM) research indicated that it would be unlikely for overpressures exceeding 138 kPa to occur very far from the

explosion origin, provided that the area on either side of the seal contained sufficient incombustible and minimal coal dust accumulations (Mitchell, 1971). Pressure balancing across the seals plays a key role in seal deployment strategies by minimising the exchange of gases and limiting the resulting volume of flammable gas in the gob.

Many countries, including the US, Australia, France, Germany, Poland and China, have pursued or are pursuing research for developing and evaluating explosion-resistant structures for sealing sections of underground mines. Australian investigators (Pearson *et al*, 2000) are considering new approaches to the design and evaluation of mine stoppings and seals including performance testing and use of computer programs for structural behaviour analysis. Since the early 1990s, NIOSH and MSHA have been jointly investigating the ability of various existing and new seal designs, to meet or exceed the requirements of CFR. Before any new seal design type can be deemed suitable by MSHA for use in underground coal mines, the seal design is generally required to undergo full-scale performance testing at PRL's LLEM (Triebsch and Sapko, 1990).

Shown in Figure 1 is the multiple entry section of the LLEM which has been used to performance test various seal designs for compliance with 30 CFR. Most of the seals were constructed in the cross-cuts between B- and C-drifts. These cross-cuts were approximately 2 m high by 5.8 m wide. The average cross-sectional area of the cross-cuts was 11.6 m². Prior to the test, a concrete/steel bulkhead was positioned across E-drift to contain the explosion pressures within C-drift. For the explosion tests, methane was injected into the closed end of C-drift (Figure 1). A plastic diaphragm contained the methane-air mixture within the first 14 m. A fan, with an explosion-proof motor housing, mixed the methane and air. The ignition of the nine to ten per cent methane-air zone generated a peak pressure pulse of approximately 140 kPa as the explosion propagated down the entry. This peak pressure pulse, measured at the wall perpendicular to the direction of propagation, remained relatively constant throughout the length of the seal test zone in C-drift.
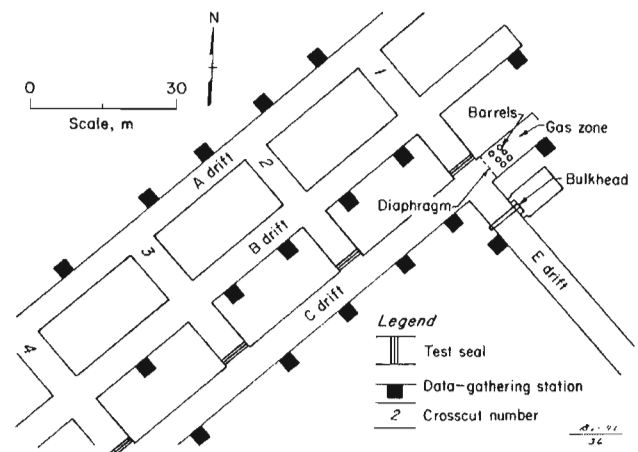

FIG 1 - Seal test area in the LLEM.

1. National Institute for Occupational Safety and Health, Pittsburgh Research Laboratory, PO Box 18070, Pittsburgh PA 15236, USA.

Many seals appear to be mostly intact after the explosion but are unable to properly limit the exchange of air. Therefore another important factor which is considered as part of the acceptance criteria is the seal's ability to prevent, or reduce, the exchange of gases from one side of the seal to the other. Measurements of the air leakages across the seals are conducted before and after the explosion tests and compared to the MSHA-established guidelines. These guidelines are as follows: for pressure differentials up to 0.25 kPa, air-leakage through the seal should not exceed 2.8 m^3/min; for pressure differentials over 0.75 kPa, air leakage should be less than 7.1 m^3/min. Many seal designs have withstood the required 138 kPa explosion pressure, with little visual damage, but failed the subsequent post-explosion leakage criteria. Description of the window technique for measuring pre- and post-test leakage is presented by Greninger *et al* (1991).

This full-scale explosion testing is very elaborate, time-consuming, costly and often conflicts with other high priority research conducted at the Lake Lynn facility. The current work is aimed at developing acceptable alternative methodologies to better characterise strength properties of mine seals and their ultimate interaction, within the mine geology. NIOSH constructed two test chambers within the LLEM and one within the SRCM to compare the static and dynamic response of candidate seals, to different forms of pressure loading including water, compressed air, and the combustion products from internal explosions of methane-air. Data from these chamber studies were used to compare the strength characteristics, with the same seal designs previously tested against full-scale 140 kPa psi explosions, within the LLEM. These chamber experiments also provide data for the ultimate failure pressure and for developing generalised geometric size scaling relationships, for predicting seal performance as a function of entry cross-section.

This paper provides an overview of NIOSH research to evaluate the use of a test chamber concept, for pressure loading of full-size seals using compressed air, water, or internal gas explosions.

Test chamber approach

Two large-scale underground chambers were constructed within the LLEM to conduct pneumatic, hydrostatic, or explosion pressure loading of candidate seals. Figure 2 is a schematic of the chamber design. The large chamber dimensions are 9.1 m wide by 4.6 m high by 3.1 m deep with a maximum cross-sectional area of 42 m^2. The smaller of the two chambers is 6.1 m wide by 2.4 m high by 3.1 m deep and can accommodate a seal design, with a cross-sectional area up to 15 m^2 (Sapko *et al*, 1999; Sapko, Weiss and Greninger, 1999; Sapko and Weiss, 2001; Sapko, Weiss and Harteis, 2003).

Both chambers were connected via remote-controlled air valves to two diesel-driven air compressors which provided 28 m^3/min of air. The air compressors were used to conduct the pre- and post-explosion leakage measurements and to pressure load some seal designs up to 140 kPa. Both chambers were connected to a 22 kW electric water pump, capable of 6.3 L/s at 690 kPa at the chamber inlet, with water fed from an underground 500 m^3 reservoir. When the water leakage from the test seal exceeded the capacity of the electric water pump, a diesel driven water pump capable of supplying up to 3.78 m^3/min at 690 kPa was used to conduct the experiment.

Each chamber was equipped with methane and oxygen injection systems and an internal mixing fan for conducting methane-air explosion studies. The oxygen and the methane were supplied by compressed gas cylinders. A pre-determined amount of 99.9 per cent methane was metered into the chamber and thoroughly mixed with the air, using a fan located within the sealed area of the chamber. The fan generates an airflow of 85 m^3/min. Uniformity of pre-test gas concentrations was determined by drawing gas through tubing and into an on-line infrared methane analyser and a para-magnetic oxygen analyser. Samples were also collected in evacuated glass tubes for subsequent analysis by gas chromatography. The flammable gas mixture was ignited at the centre of the combustible volume by an 0.5 s electrical discharge from a 30 kV luminous tube transformer, across a 3.2 mm spark plug gap. The combustion of pre-mixed methane-air mixtures within the chamber produced gas overpressures sufficient to cause ultimate failure/rupture of the seal.

The two chambers were equipped with internal 0 - 1.4 MPa strain gauge pressure transducers (1000 Hz) for measuring the internal explosion pressure history. Three spring-loaded linear variable displacement transducers (LVDT) were mounted around a 90 degree bend outside the chamber and connected to the test seal via lightweight, near zero stretch (fishing) line. This mounting system protected the expensive LVDTs from flying seal fragments. One LVDT was connected at the exact centre (mid-height and mid-width) of the seal. A second LVDT was connected at the 1/4-height and mid-width point. A third LVDT was connected at the 3/4-height and mid-width point. As the seal was pressure loaded, the seal displaced outward and the LVDTs measure this displacement by generating an output signal of approximately 65.6 mV/mm. Data were recorded at 2000 samples per second, per channel, with a WINDAQ PC-based data acquisition system.

Chamber pre- and post-test leakage

Although many of the standard seal designs appeared to be mostly intact after the confined explosion within the chamber, some seals were later shown to be unable to properly limit the exchange of air from one side to the other. The conventional method, for measuring air leakage through seals explosion tested within the LLEM, involves measuring, with an anemometer, the air that passes through the seal and through a 465 cm^2 window in a nearly air-tight brattice curtain installed downstream of the seal, while maintaining a constant differential pressure across the seal (Greninger *et al*, 1991).

Air leakage from the chamber was determined by recording chamber pressure decay, as air leaked through the seal. Compressed air was used to initially raise the pressure to about 1.2 kPa and when stopped, the pressure in the chamber behind the seal began to decay. Results from the pressure decay method were compared with the conventional window method. While
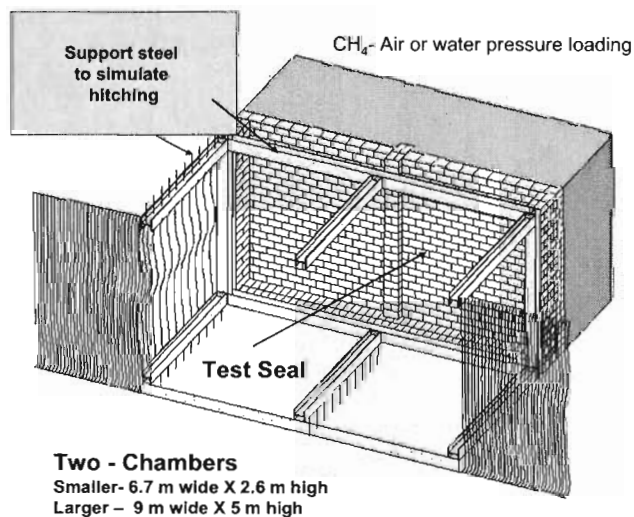

FIG 2 - Large test chamber for pressure loading of seals with water, compressed air and with the combustion of confined concentrations of methane-air.

Support steel to simulate hitching

CH$_4$- Air or water pressure loading

Test Seal

Two - Chambers
Smaller- 6.7 m wide X 2.6 m high
Larger – 9 m wide X 5 m high

details of the development of the pressure decay method for measuring air leakage can be found in Sapko *et al* (2003), only the final equation is presented here.

The volumetric loss rate, Q, can be calculated as follows:

$$Q = -\frac{V_o}{\gamma}\frac{C_w}{P}\frac{dP}{dt} \qquad (1)$$

where:

Q   = volumetric loss rate from chamber, m^3/s

V_o is void volume behind the seal, m^3

γ = 1.4 for air

P   = chamber pressure, kPa

dP/dt   = decay rate at pressure P, kPa/s

C_w = assumed discharge coefficient

Comparisons between Equation 1 pressure decay and the steady state window leakage technique as used for the LLEM explosion tests agree, within ten per cent, using a discharge coefficient of 1.0. This pressure decay method for air leakage measurements is much easier to use, since it does not require the installation of an air tight membrane and window in front of the test seal.

Tests, in which water pressure was used to load the seal, suggest that a relationship should exist between the maximum water leakage rate during the test and the post-test air leakage, providing that the leakage pathways/cracks do not significantly change after the load is removed and the seal relaxes. Figure 3 shows the correlation between maximum water leakage measured during loading with the post-test air leakage measurements at 0.25 kPa differential pressure for standard and cementitious type seals. This relationship may not hold for other seal designs since water leakage pathways may change significantly with seal designs using composite type or more elastic type materials that relax after loading. For these situations, the air pressure decay approach would be the method of choice for determining air leakage.
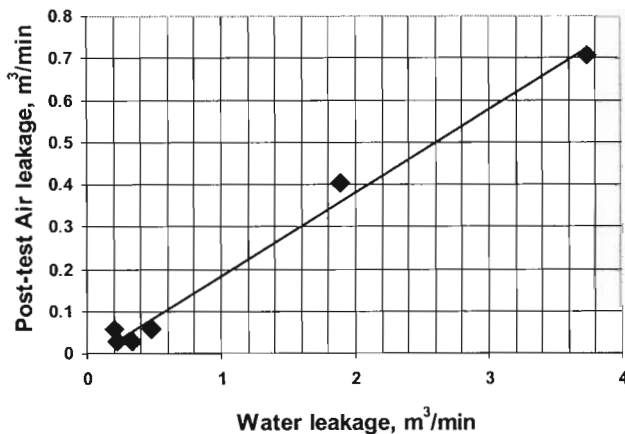
FIG 3 - Comparison of post test air leakage with maximum water flow.

Types of seals tested

Several of the seal designs evaluated previously in C-drift and in this chamber study are shown in Figure 4. These seal designs, with the test designations in parentheses, include the standard-type, solid-concrete-block seal (C1, C2, C6, and L1), the pumpable cementitious plug design (C3, C7, and L2), the
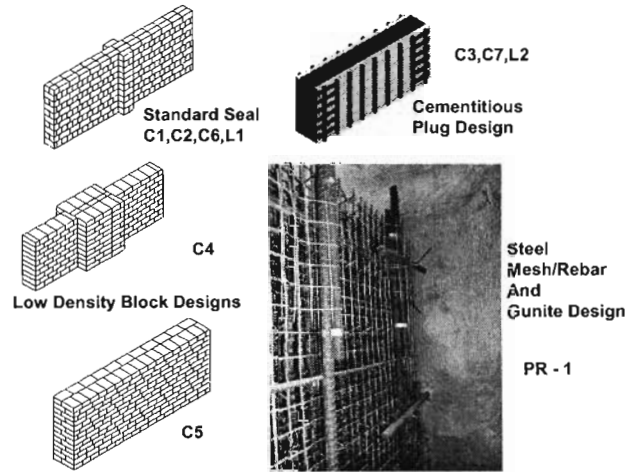
FIG 4 - Various types of seal designs tested in the new chambers.

low-density block seal designs with (C4) and without pilasters (C5), and the steel mesh and gunite design (PR-1). These seal designs have been deemed suitable by MSHA for use in underground US mines based on full scale explosions tests in the multiple entry LLEM.

The standard-type, solid-concrete-block seal design was chosen for the initial evaluation, since this design was extensively evaluated over several years in the PRL's SRCM and in the LLEM. In fact, this standard-type seal was used to form the basis for the current regulations (30 CFR, Part 75.335). Of the solid-concrete-block seals tested in the experimental mines, only the standard-type seal design – 406 mm thick with staggered and fully mortared block joints, a centre pilaster, floor and rib keying (hitching), and wedged at the roof (Figure 3 – C1) – successfully withstood the required 138 kPa pressure pulse. This same seal design was installed in both the small and large chambers for most of the comparison studies.

The three other seal designs (Figure 4) were also performance tested using the chamber approach. Exposing these seals to methane-air explosions, within the large and small chambers, allowed for the determination of the ultimate failure pressure and provided data for developing geometric size-scaling relationships. The determination of the ultimate failure pressure is not a performance requirement of 30 CFR, but such data will provide seal manufacturers and mine operators with an estimate of design safety factors for a particular seal design.

Water pressure loading

Hydrostatic (water loading) tests were also conducted on two standard-type, solid-concrete-block seal designs. One seal, with a 5.5 m wide by 2.4 m high unsupported span between the centre pilaster and each rib, was located in the small chamber within the LLEM. The other seal, having a similar 5.4 m wide by 2.4 m high unsupported span, was located in a 'butt' entry of the SRCM. The chambers within the LLEM are constructed in a solid unyielding limestone formation, while the 'butt' entry in the SRCM is within the Pittsburgh coal seam.

Figure 5 is a schematic of the finished seal as constructed in the SRCM. Hitching of the seal required the removal of about 0.25 m of crushed limestone from the mine floor to expose the solid coal base. This crushed limestone was used to control water accumulations in the SRCM. A 0.15 m thick by 0.6 m wide concrete footer (approximately 21 MPa compressive strength) was constructed on the solid coal floor to provide a base for the seal. A 0.5 m wide by 0.15 m deep channel was cut vertically into both ribs to provide hitching. The small gap between the mine roof and the top of the seal was filled with Quikcrete

Gunite (16.9 ± 2.4 MPa compressive strength). Both sides of the seal were coated with a latex-based waterproofing sealant, to minimise water leakage during pressure loading. The chamber behind the seal was then filled with water.

During the filling process, the displaced air within the chamber area was vented using a pipe extending through and near the top of the seal; one end of the pipe was located at the highest position within the chamber area behind the seal. When water was observed venting through the pipe, the air vent valve was closed, allowing the water pressure behind the seal to continue to increase.

Figure 6 shows the pressure history, as recorded from a transducer located on the seal about 1.5 m above the floor, while the water flow rate was held relatively constant at 5.7 L/s. As the water displaced the air behind the seal, the pressure within the chamber began to rise. The pressure peaked at 218 kPa when the pump was stopped. The pressure then began to decay through various cracks in the mortar. After the pressure decayed to about 125 kPa, a 5 cm diameter drain pipe valve was opened resulting in more rapid pressure decay.

Several tests, comprised of increasing water pressure loadings, were conducted on each smaller seal design. Following each test, the water was drained and post-test air leakage evaluations were conducted. For all cases, the post-test air leakage measurements were well within acceptable limits. Table 1 contains the results of these water pressure tests on the standard-type, solid-concrete-block seals, one installed in the SRCM (SRCM 1) and the other in the small chamber located within the LLEM (C6-60). Note that the 1.89 m high SRCM 1 seal, hitched within the coal seam, deflected about 3.6 mm at-roof pressure load of 138 kPa. In contrast, the 2.62 m high standard seal constructed within LLEM test limestone chamber only deflected about 0.25 mm. This result demonstrates the importance of roof to floor stiffness to resist the thrust generated by arching action for those seals that gain their ultimate strength through arching action between the roof and floor. Although the SRCM 1 seal was not tested to destruction, its ultimate strength is assumed to be less than those constructed with unyielding abutments. Also listed in Table 1 are the small chamber test results (C7-70) for a 1.2 m (48 in) thick cementitious type plug seal with an average compressive strength of 1.75 MPa.
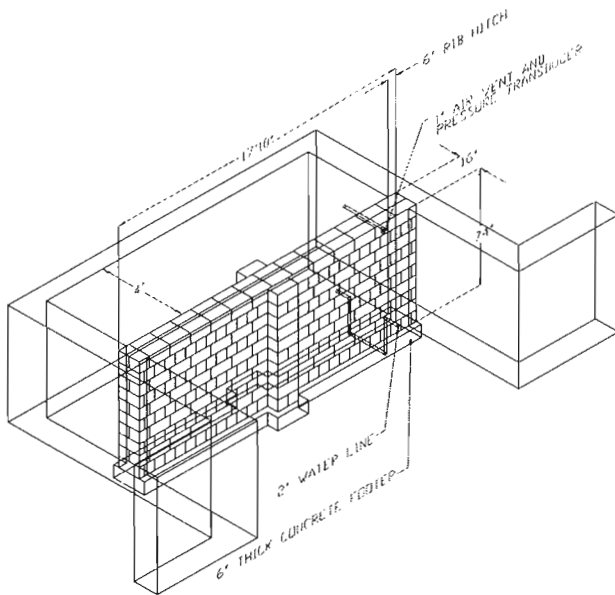

FIG 5 - Schematic of the SRCM used for water loading the standard-type seal design with pilaster.

TABLE 1

Centre deflection of various seals at 138 kPa water pressure loading.

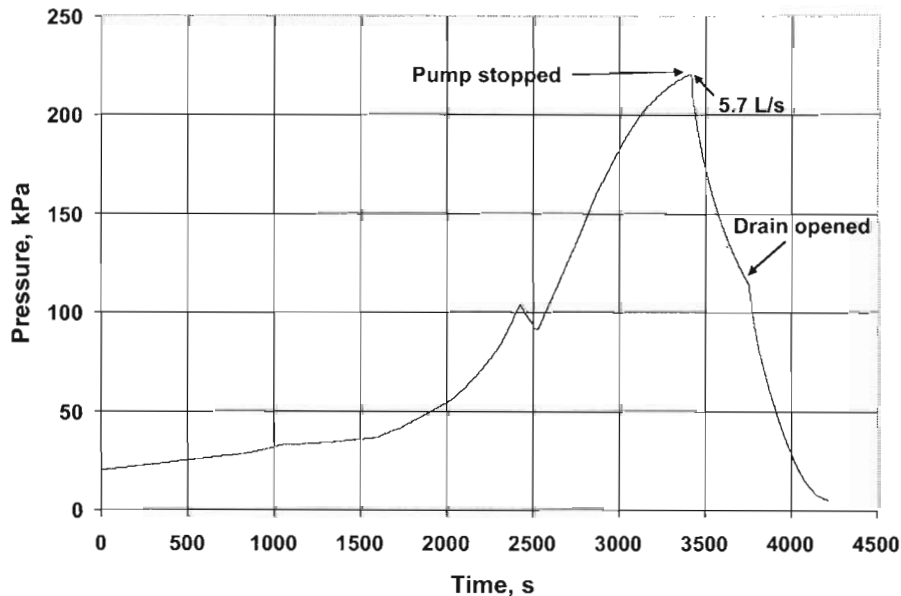| Seal test	Width (m)	Height (m)	Thickness (m)	Mid seal deflection at 138 kPa roof water pressure (mm)
Standard-type, solid-concrete-block seal				
C6-60	5.14	2.62	0.4	0.25
SRCM 1	5.49	1.89	0.4	3.6
Cementitious pumpable plug seal				
C7-70	6.46	2.66	1.22	5
Gunite/rebar steel mesh seal				
PR-1	6.4	2.6	0.28	1
SCRM – Safety research coal mine hitched in Pittsburgh coal seam				

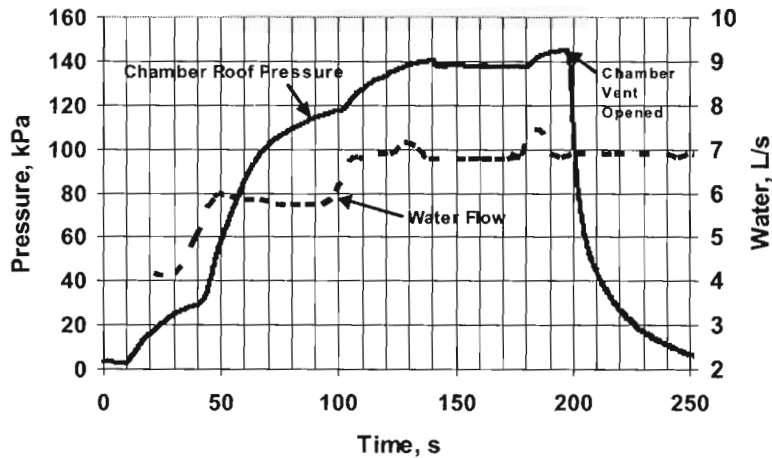FIG 6 - Water pressure history for the standard-type seal design tested in the small LLEM chamber.

FIG 7 - Water flow and pressure loading histories for the standard-type seal design tested in the SCRM coal seam.

Figure 7 shows the pressure history and water flow rate for the SRCM water test on the standard seal design. This test achieved a maximum flow rate of approximately 7.6 L/s, which produced a peak pressure of about 145 kPa at the roof of the chamber. Owing to the hydrostatic head, the pressure at the base of the seal was about 172 kPa. With gas pressure loading, however, the pressure across the seal is uniform. Thus while water loading is easier to carry out in terms of *in situ* measurements, there will always be a difference in pressure between the roof and floor due to the hydrostatic water head of 10.1 kPa per metre of seal height.

Although in both cases (SRCM and LLEM chamber) the water capacity was insufficient to determine ultimate strength, as defined by the failure of the post-test air leakage, it was adequate to demonstrate the seals' ability to resist the required 138 kPa pressure loading. This water flow limitation is not perceived to be a problem for testing within the actual mine environment, where the underground water supply from the surface will be driven by the large hydrostatic heads, fed through large diameter pipes, or in situations where diesel driven booster pumps are available.

Since available water supplies were insufficient for determining the ultimate failure pressure, internal chamber explosions of methane-air mixtures were used to produce over pressures up to 690 kPa, sufficient for loading all test seals to ultimate failure. These explosion tests also provided data to compare the response of the same seal design to both dynamic (rapid pressure buildup) and static (slow pressure buildup) loading.

CHAMBER EXPLOSION TESTS

To determine the ultimate failure pressure of various seal designs, methane-oxygen mixtures were injected into the void volume behind the various types of seals and then ignited in the centre of the confined chamber. Obviously, this type of evaluation test using methane is intended only for controlled experimental research and not intended for use in coal mines.

Shown in Table 2 is a summary of seal dimensions and explosion test results. Several explosions of varying intensity were conducted in the small chamber against the standard-type, solid-concrete-block seal with a centre pilaster (seal C1 in Table 2). Four explosions were also conducted against a modified standard seal design (seal C2 in Table 2) that did not include a centre pilaster. In addition to the small chamber tests, a standard-type seal design with a centre pilaster was tested to failure in the large chamber (seal L1 in Table 2). To evaluate the size-scaling issues, this large chamber seal was constructed to the same thickness as the small chamber seal.

TABLE 2

Summary of seal dimensions and explosion test results.

Seal test	Width (m)	Height (m)	Thickness (m)	Max Chamber Pressure (kPa)	Result
Standard-type, solid-concrete-block seal[*]					
C1-5[1]	5.14	2.62	0.4	390	DNR
C1-8[1]	5.14	2.62	0.4	622	DNR
C1-9[1]	5.14	2.62	0.4	651	DNR
C1-10[1]	5.14	2.62	0.4	549	DNR
C1-11[1]	5.14	2.62	0.4	688	R
C2-24	5.14	2.62	0.4	518	DNR
C2-25	5.14	2.62	0.4	524	DNR
C2-27	5.14	2.62	0.4	538	DNR
C2-29	5.14	2.62	0.4	669	R
C6-62[1]	5.53	2.4	0.4	600	DNR
L1-35	8.53	4.72	0.4	221	R
Low-density block seals					
C5-53	6.27	2.68	1.02	124	R
C4-48[2]	6.09	2.49	0.6	152	R
Cementitious pumpable plug seals					
C3-44	6.46	2.66	1.22	221	R
L2	9.4	4.75	1.22	90	R

DNR   Did not rupture
R   Ruptured
1   Pilaster 16 inches wide by 32 inches deep
2   Pilaster 72 inches wide by 32 inches deep
*   20 × 15 × 40 cm solid concrete block. Average block compressive strength is 17.9 ± 0.69 MPa.

The standard-type seal C1, withstood four constant volume explosions before it ruptured at a peak static pressure of 688 kPa. The first four tests (C1-5, C1-8, C1-9, and C1-10 in Table 2) subjected the seal to pressure loadings ranging from 390 kPa to 651 kPa. It was only after the C1-9 test (651 kPa) that hairline cracks were visible along the central mortar joints. The post-explosion leakage rates did increase to about 2.7 m³/min at 0.25 kPa, which was still within the acceptable limits. To further increase the pressure loadings for the C1-11 test, ~6 m³ (210 ft³) of oxygen was first injected into the chamber followed by the methane resulting in a near stoichiometric ratio of 13 per cent methane mixture.

Three of these explosion pressure loading histories recorded for the standard seal C1 are shown in Figure 8 to illustrate the large differences in the rate of pressure loadings. The combustion of six per cent methane-air mixture, the slowest burning rate, peaked at about eight seconds at 390 kPa while the most rapid burning rate with added oxygen peaked at 0.34 seconds at 688 kPa. Shown in Figure 9 is the corresponding centreline deflection for the three explosions. The deflection increases linearly with increasing pressure at a nearly constant rate of 0.003 mm/kPa for all three explosions. Also shown in Figure 9 is the response of the standard seal design C6 to water loading. In this case, the water pressure peaked out at 200 kPa after 45 minutes. The centreline response of the standard seal is nearly the same over these extreme rate of load application differences which indicates that resistance of the seal is largely independent of inertial effects. Interestingly, in the 1920s the Bureau of Standards (BOS) conducted static and explosive tests for the USBM on concrete stoppings and hypothesised that, 'it would be expected that the loading stresses caused by explosive pressures would not differ appreciably from bending stresses produced by static pressures of the same magnitude...' Based on their experimental results, the BOS hypothesised that '...inertia effects would be negligible'. The results of these experiments support the BOS premise that static and dynamic bending stresses would be similar. Even though the deflection of the seal varies with time, the response can be predicted by static analysis consistent with the 30 CFR 138 kPa static pressure requirement.
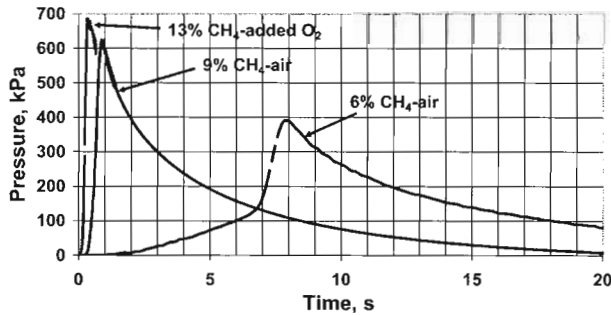

FIG 8 - Chamber explosion pressure histories recorded during testing of standard seal C1 in the small chamber to failure.
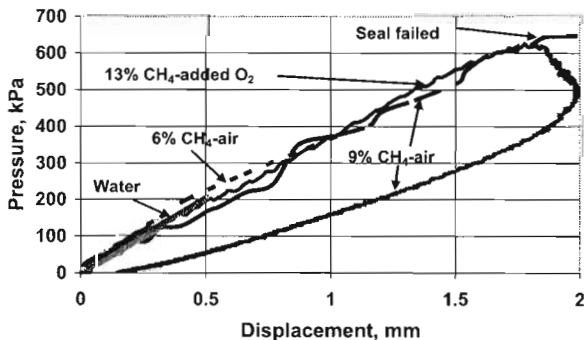

FIG 9 - Standard seal deflection as a function pressure loading.

The remains of seal C1 after rupture are shown in Figure 10. The centre of the seal was blown out while part (152 mm thick by 406 mm wide) of the pilaster on the explosion side remains. The almost conical-shaped perimeter shear pattern is visible in
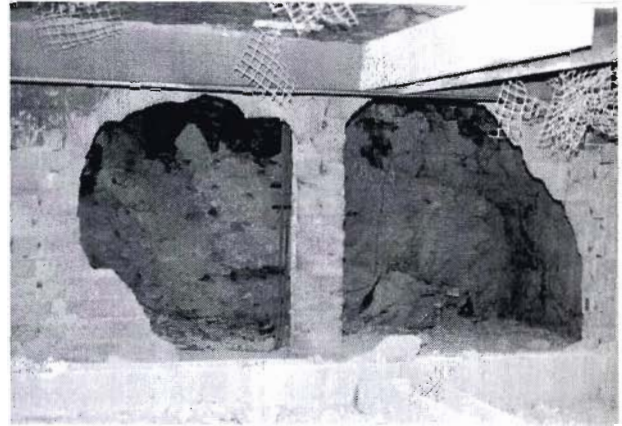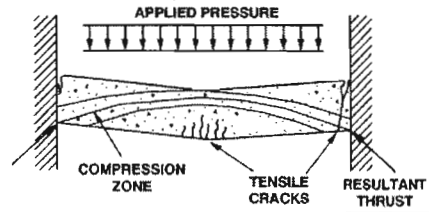

FIG 10 - Remains of the standard-type seal when exposed to 688 kPa pressure loading produced from the combustion of a methane-air-oxygen mixture.

the remains of the seal, indicating an arching failure pattern. As the seal deflects under load, changes in geometry cause the edges to move outward, pushing against the rigid limestone.

Shown conceptually in Figure 10 are the compression zone and resultant thrust that develops from this reaction, when laterally restrained by unyielding roof- floor-rib abutments. Seal C2, without the centre pilaster, ruptured during the fourth explosion at a peak static pressure of 669 kPa, or ~20 kPa below the failure pressure of seal C1 with the centre pilaster. Both seals provide a margin of safety of about 4.8 to five times the CFR requirement when restrained between 34.5 MPa concrete floor and 113 MPa limestone roof. Unless the mine site roof-floor conditions are the same as these experimental conditions (≥34.5 MPa), this same margin of safety may not be realised. Also, in an underground mine, post construction floor to roof convergence may add significant compression stress to the seal. This pre-stressed condition may reduce the strength of the seal, since less pressure would be required to increase the stress in the masonry to the point, where it crushes during the arching action.

A mixture of 5.7 per cent methane-air was ignited in the large chamber with a 41 cm thick standard seal. The chamber pressure rose rapidly to about 222 kPa in 13 s and then rapidly decayed to zero as the combustion gases vented through fractures, which formed as the seal began to break up and displace outward. The midpoint displacement of the seal as a function of pressure loading is shown in Figure 11. The midpoint of the seal displaced linearly with increasing explosion pressure up to about 12 mm deflection at ~207 kPa. The chamber pressure continued to increase to about 222 kPa, remaining relatively constant, until the midpoint of the seal displaced about 71 mm the maximum range of the LVDT. At 71 mm, chamber gases rapidly vented through the fractured seal and the chamber pressure rapidly dropped to zero. In this example, the ultimate failure pressure for this seal was selected 207 kPa, where the seal ability to resist pressure fails rapidly. This approach was used to determine the ultimate failure pressure for each seal and provided necessary data to develop the following size-scaling relationships.
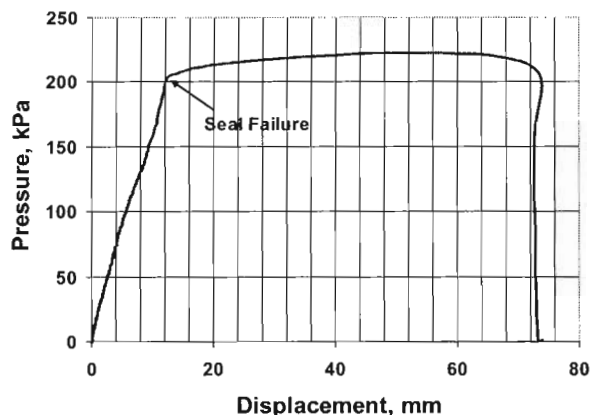
FIG 11 - Pressure loading of standard-type seal in large chamber as a function of centre displacement.

Test method comparison

Before an alternative approach for performance testing is considered for new seal designs, a comparison of both test methods using the same seal designs must first be conducted. Five seal designs that passed the 138 kPa static explosion test in C-drift of the LLEM and, subsequently deemed suitable for use by MSHA were also tested in the small chamber. Shown in Table 3 are the results of this comparison. All five seals that passed the LLEM full-scale 138 kPa *static* pressure explosion test also passed the small chamber test. Although not required by the current 30 CFR approval process, the chamber approach also provides a means to determine the ultimate strength of the seal design for the same test conditions. Even though all designs were capable of resisting the 138 kPa load, some designs were capable of resisting much higher pressures.

SIZE SCALING OF SEALS

In the early 1930s, the USBM conducted a series of tests and found that restraining the edges of a seal caused a dramatic increase in the seal strength to a much higher level, than predicted by plate theory (Rice, Greenwald, and Howarth, 1930; Rice *et al*, 1931). Full-scale explosion experiments also showed concrete walls that were recessed into the roof, ribs and floor, and had a thickness to width ratio of at least 0.1, resisted much higher pressures than the theoretical design pressure. Their results showed that recessing the ends of the concrete wall into the surrounding strata, allows the wall to act as a flat arch. This arching behaviour transmits a lateral thrust to the strata, which then act as a buttress to prevent seal movement. Several efforts have been made to explain the arching behaviour through various static design models.

McDowell showed that arching can be used to explain the significantly higher lateral loads that brick beams are capable of withstanding than conventional bending beam analysis would allow (McDowell, McKee and Sevin, 1956). McDowell proposed that a three-hinge arch is formed and that the resistance of the wall to lateral loading is due entirely to the tendency of the masonry to crush at the mid span and end supports, due to the arching action. Immediately upon loading, cracks develop on the tension side at the ends and centre of the span. Initially, these cracks extend to the centreline of the beam (wall). During subsequent motion, it is assumed that each half of the wall remains rigid and rotates about an end and where the two half walls meet at the centre of the wall. The resistance to this motion comes about through a force couple set up at the ends and centre due to crushing of the masonry at these positions. The rotation continues until the resisting couple vanishes (ie the material fails) or the load is removed.

McDowell also reported on a series of tests conducted at the Massachusetts Institute of Technology, where 17 brick beams were tested under fixed-end conditions (Massachusetts Institute of Technology, 1954). These tests were consistent with the arching theory. The ultimate strength of the beams was shown to correlate to the compressive strength of the material. The transverse load capacity was six times greater than what a simply supported beam analysis predicts.

Anderson (1984) examined the theory of arching in more detail by comparing the behaviour of masonry walls during the initial loading prior to cracking of the wall and post-cracking behaviour of the wall. He concluded that the load required to cause cracking of a wall with rigid abutments can be three times greater than a wall without arching restraint. Anderson developed an equation relating the arching thrust to the transverse load. Through these and related efforts, arching has been recognised as a valid loading mechanism and design consideration for walls bridging rigid abutments. The British Codes of Practice (British Standards Institution, 1978) first recognised arching as a design mechanism in 1978.

The simple three-hinged arch theory used as the basis of the BS5628 formula was expressed by Anderson 1984 in its ultimate load terms as

$$w = 7.2 \, P_u \, t / L^2 \qquad (2)$$

This is a convenient formula to use to compare the effect of parameters using the same value P_u. P_u is defined as the limiting arching thrust that induces a uniform stress over a depth of $2 \, t \, (0.5 - e/t)$.

$$P_u = 2 \, t \, n \, f_k \, (0.5 - e/t) \qquad (3)$$

Combining Equations 2 and 3, one obtains the following expression for the ultimate load used for size-scaling data from this study.

TABLE 3

Comparison of results from the proposed new chamber test method with current full-scale explosion test method.

Seal type	LLEM 138 kPa explosion loading	Small chamber 138 kPa water or air loading	Ultimate strength (kPa)
Standard seal C1	Passed	Passed	690
Standard seal without pilaster C2	Passed	Passed	538
Cementitious plug seal C3	Passed	Passed	220
Steel mesh and gunite PR-1	Passed	Passed	>214
Low density block C4	Passed	Passed	152

$$w = 14.4 \, n \, f_k \, (0.5 - e/t) \, (t/L)^2 \qquad (4)$$

where:

w = ultimate load, kPa

L = the height of the seal, (smaller dimension) m

t = the thickness of the seal, m

f_k = the compressive strength of the seal material, kPa

e = the eccentricity of arching thrust = 0.45 t

n = stress factor-based on the ratio of the unit strength to the ultimate strength in the hinges (Anderson, 1984) $n = 0.75$ brickwork to 1.25 for block work

Close contact between the seal and roof must be maintained for these criteria to be applicable. In this study, the 1 to 3 cm gap between the top block course of the standard seal and roof is filled with type S mortar to provide effective roof to seal coupling and ensure arching action. During construction of the pumpable cementitious type seals, the material is pumped under pressure into the form to ensure complete contact with the roof.

$$w = 0.72 \, n \, f_k * (t/L)^2 \qquad (5)$$

If the roof and floor strength are weaker than the compressive strength of the material used to construct the seal, then the lower value should be used for f_k to estimate the ultimate strength of the seal.

Shown in Figure 12 are the experimental results from the chamber testing of the standard seal and standard seal without the pilaster for both large and small chambers constructed with solid blocks with a measured average compressive strength of 17.9 MPa. The best fit straight line through two small seals, the large seal that failed and zero is based on the simplified formula for arching in the transverse laterally loaded wall using Equation 5 and solving for an effective n; $n = 1.82$ from these studies. Shown in Figure 13 are the experimental results from the chamber testing of the pumpable cementitious seals, for both large and small chambers, constructed with material with an average compressive strength of 1725 kPa. Similarly, the same approach was applied to the plug seal data. Although the plug seal data is more limited, the best straight line fit produces an $n = 0.76$.

Results from these studies with the standard seal design suggests an ultimate strength size-scaling relationship of $w = 1.3 \, f_k \, (t/L)^2$ for seals ≥41 cm thick and seal height L between
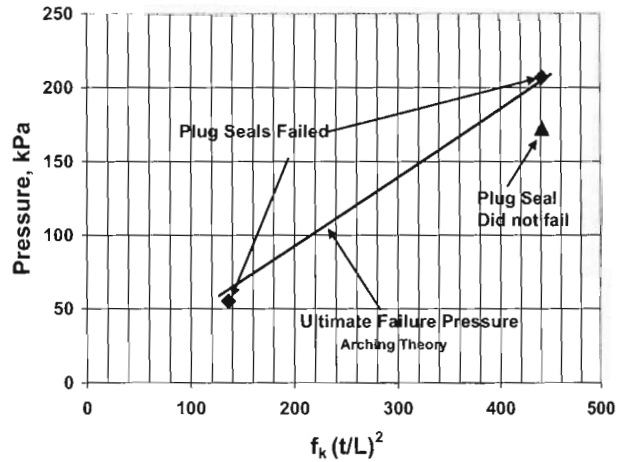
FIG 13 - Size-scaling of the ultimate seal strength for the cementitious type plug seals ≥120 cm thick using arching theory.

1.8 and 5 m. Studies indicate a size scaling relationship of ultimate strength for cementitious type plug seal designs of $w = 0.55 \, f_k \, (t/L)^2$ for thickness ≥120 cm and heights L between 1.8 and 5 m.

Although the agreement with experimental data is fairly good, this approximation for ultimate seal strength should be used with caution. The accuracy of the prediction relies on quality masonry construction, close contact between the seal and the floor/roof abutments, and that the abutment thrusts are higher than the values to cause crushing of the masonry (17.9 MPa) under arching action.

Assuming quality seal construction adapted to the mine environment, these results suggest that the arching theory provides a reasonable method for size scaling the ultimate strength of mine seals with rigid abutments.

SUMMARY

Before MSHA will deem a seal design suitable for use in underground coal mines, the design has to be evaluated and, in most instances, undergo explosion testing within the LLEM. Results from this study indicate that a static design analysis coupled with an *in situ* hydrostatic approach shows promise as an alternative method for performance testing seals that would be consistent with the intent of the 30 CFR, 20 psi (138 kPa) static
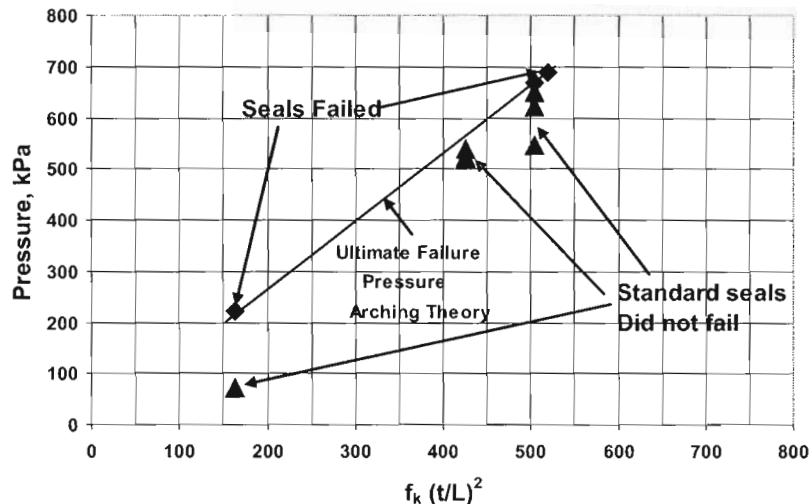
FIG 12 - Size-scaling of the ultimate seal strength for the standard seals ≥40 cm thick using arching theory.

pressure requirement. The new *in situ* approach is most effective, when the design analysis and performance testing is validated within the particular mine geology. The conditions that might exist in one mine will likely vary within a mine and between mines, therefore the use of conventional design tools coupled with occasional *in situ* testing to verify performance would be one approach for the regulatory authority to consider in approving new seal designs. Some non-conventional seal designs consisting of sandwiched layers of composite material may require more performance testing to develop and validate acceptable design models.

Geometric size-scaling relationships based on arching theory and non-yielding abutments are presented for standard seal and cementitious plug seal designs for predicting ultimate strength. These relationships for predicting ultimate seal strength should be used with caution. The accuracy of the prediction relies on quality construction, good coupling between seal and roof, and assumes that the abutments thrusts are higher than the values to cause crushing of the seal material during arching action between the seal roof and floor.

Acceptance of this alternative *in situ* water loading approach, coupled with the ability to determine the ultimate failure pressure of the seal, should facilitate the development and implementation of stronger reliable seals, and thereby enhance the level of protection for underground personnel.

ACKNOWLEDGEMENTS

REFERENCES

Anderson, C, 1984. Arching action in transverse laterally loaded masonry walls, *The Structural Engineer*, 62B(1):22.

British Standards Institution, 1978. BS 5628, Code of practice for the structural use of masonry: part 1; un-reinforced walls (British Standards Institution: London).

Greninger, N B, Weiss, E S, Luzik, S J and Stephan, C R, 1991. Evaluation of solid-block and cementitious foam seals, USBM RI 9382, 13 p.

Hurren, W E, Tuggle, G N and McGruder, F I, 1993. Mary Lee No 1 Mine, Accident investigation report, underground coal mine, August (US Labor Dept MSHA).

Massachusetts Institute of Technology, 1954. Behavior of walls panels under static and dynamic loads II (Department of Civil and Sanitary Engineering).

McDowell, E L, McKee, K E and Sevin, E, 1956. Arching action theory of masonry walls, *Proceedings of the American Society of Civil Engineers*, Paper 915, Journal of the Structural Division, 82(ST2):915-1-915-18.

Mitchell, D, 1971. Explosion-proof bulkheads: present practices, USBM RI 7581, 16 p.

Parsons, D E, 1922. Tests of mine stoppings under static and explosive pressures, Bureau of Standards technical report.

Pearson, D, Gillies, A D S, Green, A, Ray, R and Dux, P, 2000. New approaches to the design and evaluation of mine stoppings and seals, in *Proceedings 2000 Queensland Mining Industry Health and Safety Conference*, Townsville, August, pp 309-325.

Rice, G S, Greenwald, H P and Howarth, H C, 1930. Tests of the strength of concrete stops designed to resist the pressure of explosions in coal mines, USBM RI 3036, September, 11 p.

Rice, G S, Greenwald, H P, Howarth, H C and Arins, S, 1931. Concrete stops in coal mines for resisting explosions: detailed tests of typical stops and strength of coal as a buttress, *USBM Bull*, 345:55-57.

Sapko, M J and Weiss, E S, 2001. Evaluation of new methods and facilities to test explosion-resistant seals, in *Proceedings 29th International Conference of Safety in Mines Research Institutes*, Katowice, Poland, October, Vol 1, pp 157-166.

Sapko, M J, Weiss, E S, Cashdollar, K L and Greninger, N B, 1999. Overview of NIOSH's mine seal research and future plans, in *Proceedings 28th International Conference of Safety in Mines Research Institutes*, June, pp 71-85.

Sapko, M J, Weiss, E S and Greninger, N B, 1999. Recent mine seal research conducted by NIOSH, in *Proceedings of the Sealbarr'99*, Katowice, Poland, May, pp 39-53.

Sapko, M J, Weiss, E S and Harteis, S P, 2003. Alternative methodologies for evaluating explosion-resistant mine ventilation seals, in *Proceedings 30th International Conference of Safety in Mines Research Institutes*, Johannesburg, South Africa, October, pp 615-640.

Sapko, M J, Weiss, E S, Trackemas, J D and Stephan, C R, 2003. Designs for rapid *in situ* sealing, in *Proceedings 2003 SME Annual Meeting*, Cincinnati, OH, February, Reprint No 03-010.

Scott, D S, Checca, E L, Stephen, C R and Schultz, M J, 1996. Oak Grove Mine, ID No 01-00851, Accident investigation report, US Labor Dept MSHA, January.

Triebsch, G and Sapko, M J, 1990. Lake Lynn Laboratory: a state-of-the-art mining research facility, in *Proceedings International Symposium on Unique Underground Structures*, Denver, CO, June, Vol 2, pp 75-1-75-21 (CSM Press).

US Code of Federal Regulations, 2004. Title 30 – Mineral Resources: Chapter I – Mine Safety and Health Administration, Department of Labor; Subchapter O – Coal Mine Safety and Health; Part 75 – Mandatory Safety Standards – Underground Coal Mines.

Weiss, E S, Cashdollar, K L, Mutton, I V S, Kohli, D R and Slivensky, W A, 1999. Evaluation of reinforced cementitious seals, Pittsburgh, PA: US Department of Health and Human Services, National Institute for Occupational Safety and Health, RI 9647.

Weiss, E S, Cashdollar, K L and Sapko, M J, 2002. Evaluation of explosion-resistant seals, stoppings, and overcast for ventilation control in underground coal mining, Pittsburgh, PA: US Department of Health and Human Services, National Institute for Occupational Safety and Health, RI 9659.

Weiss, E S, Greninger, N B, Stephan, C R and Lipscomb, J R, 1993. Strength characteristics and air-leakage determinations for alternative mine seal designs, USBM RI 9477, 21 p.

Weiss, E S, Slivensky, W A, Schultz, M J and Stephan, C R, 1997. Evaluation of water trap designs and alternative mine seal construction materials, in *Proceedings 27th International Conference of Safety in Mines Research Institutes*, New Delhi, India, Vol 2, pp 973-981 (Oxford and IBH Publishing Company).

Weiss, E S, Slivensky, W A, Schultz, M J, Stephan, C and Jackson, K W, 1996. Evaluation of polymer construction material and water trap designs for underground coal mine seals, USBM RI 9634, 16 p.